Weaver, P.P.E., Schmincke, H.-U., Firth, J.V., and Duffield, W. (Eds.), 1998
Proceedings of the Ocean Drilling Program, Scientific Results, Vol. 157

3. DETERMINATION AND CHARACTERIZATION OF VOLCANICLASTIC SEDIMENTS BY WIRELINE LOGS: SITES 953, 955, AND 956, CANARY ISLANDS[1]

H. Delius,[2] C. Bücker,[2] and J. Wohlenberg[2]

ABSTRACT

Four sites (953–956) were drilled north and south of Gran Canaria during Leg 157. The penetrated pelagic and volcaniclastic sediments can be identified by their different chemical compositions. This paper focuses on the volcaniclastic deposits that were logged in Holes 953C, 955A, and 956B. The sediments in these holes are mainly composed of hemipelagic, fine-grained nannofossil oozes with intercalations of volcaniclastic and siliciclastic sediments in Holes 955A and 956B. The frequency and nature of the volcaniclastics can be studied from wireline logs. The three chemically distinct volcanic lithologies of basalt, rhyolite, and trachyphonolite can be distinguished by geochemical logging data. Sites 953, 955, and 956 have distinct characterizations: Sites 953 and 956 show several large K_2O peaks caused by thick felsic volcaniclastic layers, whereas Site 955 has an overall low K_2O content that reflects low tephra content. The electrical measurements provide information about clast size. The coarse-grained volcaniclastic layers show higher electrical resistivities than the pelagic sediments. The magnetic log of the General Purpose Inclinometry Cartridge gives additional information on clast sizes in the basalt-dominated sections.

INTRODUCTION

During Leg 157, four sites were drilled in the volcaniclastic apron around Gran Canaria (Sites 953 through 956; Fig. 1). The volcaniclastic apron around Gran Canaria has a complex submarine and subaerial temporal, compositional, volcanic, and chemical growth history. Several volcanic and nonvolcanic phases are known from Gran Canaria. The dominant nonvolcanic lithologies recovered are pelagic clayey nannofossil ooze, nannofossil mixed sedimentary rock, nannofossil chalk, quartz silt, foraminifer sand, and foraminifer ooze. Major amounts of volcaniclastic sediments varying in chemical and mineralogical composition were produced during the Miocene basaltic shield, during the Mogán and Fataga volcanic phases between 15 and 9.5 Ma. The Miocene shield stage in the drill holes is represented by basaltic tuffs, lapillistones, breccias, and turbidites, overlain by peralkaline trachytes and low silica rhyolites. The volcanics of the Mogán phase are succeeded by trachyphonolites of the Fataga phase (Schmincke, 1976, 1982; McDougall and Schmincke, 1977; Schmincke, Weaver, Firth, et al., 1995).

In Holes 955A and 956B, a complete suite of three logging strings was successfully run (Fig. 2). In contrast, the Schlumberger Geochemical Logging Tool and the Formation MicroScanner (FMS) were not used at Hole 953C (Schmincke, Weaver, Firth, et al. 1995). The downhole measurements are described in individual site chapters of Schmincke, Weaver, Firth, et al. (1995). Here, we focus on the identification and log-derived characterization of the volcanic material, because these deposits contain important information about the evolution of this ocean island volcano.

PHYSICAL AND CHEMICAL LOG CHARACTERISTICS

The different quality (e.g., thickness and purity) of the tephra layers strongly influences the chemical as well as the physical log responses. Hole 956B is most appropriate for explaining the relation between log responses and the volcaniclastic lithology because a complete logging suite was run. Furthermore, a representative amount of distinct felsic and mafic volcaniclastic layers was drilled.

The highly differentiated tephra layers of the Mogán and Fataga phases (Mogán: 564.1–522.5 mbsf, and Fataga: 517.5–368 mbsf; Schmincke, Weaver, Firth, et al., 1995) contain significant amounts of potassium-rich mineral phases. The nonvolcanic components such as quartz, nannofossils, and chalk are practically potassium free except for clay minerals. X-ray fluorescence analyses reveal that the tephra layers contain the highest K_2O content of all lithologies, with concentrations ranging from 3.5 to 5.5 wt% (Schmincke, Weaver, Firth, et al., 1995; Sumita and Schmincke, Chap. 15, this volume). Thus, significant peaks in the potassium log are attributed to the felsic tephra layers (Fig. 3). The K_2O log shows clear boundaries for the tephra layers. The threshold of $K_2O \geq 2.1$ wt% is taken as significant and suitable for the identification of felsic potassium-rich tephra layers. Concentrations of FeO (FeO = FeO + Fe_2O_3) are highest in the basaltic tuffs, lapillistones, and breccias. FeO shows concentrations of >10 wt% (Schmincke, Weaver, Firth, et al., 1995; Schmincke and Segschneider, Chap. 12, this volume). Sediments with a high proportion of basaltic volcaniclastics are characterized in the logs by FeO contents >7 wt% and by high TiO_2 concentrations.

Volcaniclastic layers predicted by the logs are shown in Figure 3. The basaltic and felsic volcaniclastic sediments can be easily detected by the geochemical logs. The occurrence of numerous tephra layers between 390 and 560 mbsf corresponds to poor core recovery. The recovery of a volcanic deposition in Section 157-956B-31R-1 was fairly low (50 cm). The log characteristics of this layer are the high K_2O content (2.7–3 wt%) and the high resistivity (4–5 Ωm). Thus, a prominent felsic volcaniclastic layer is postulated to occur in the depth interval from 450 to 455 mbsf. The crossplot in Figure 4 shows the relation between the K_2O content and the electrical resistivity for the three main lithologies. The basaltic deposits show the highest resistivities ranging from 1.5 to 20 Ωm. The resistivity of the pelagic sediments mainly ranges between 1 and 1.5 Ωm. The deposits of the felsic volcaniclastics can be distinguished approximately from the pure pelagic sediments by values exceeding 1.5 Ωm. This fact agrees with the core description and the large clast size of both the basaltic and the felsic volcaniclastic sediments at this site.

Mainly basaltic breccia, lapillistone, and hyaloclastite tuff were recovered in the interval between 564 and 704 mbsf in Hole 956B. At least three volcaniclastic debrites are observed in the cores, whereby

[1]Weaver, P.P.E., Schmincke, H.-U., Firth, J.V., and Duffield, W. (Eds.), 1998. *Proc. ODP Sci. Results*, 157: College Station, TX (Ocean Drilling Program).

[2]Lehr- und Forschungsgebiet für Angewandte Geophysik, Rheinisch-Westfälische Technische Hochschule Aachen, Lochnerstr. 4-20, D-52056 Aachen, Federal Republic of Germany. heike@sun.geophac.rwth-aachen.de

Prior Chapter Contents Next Chapter

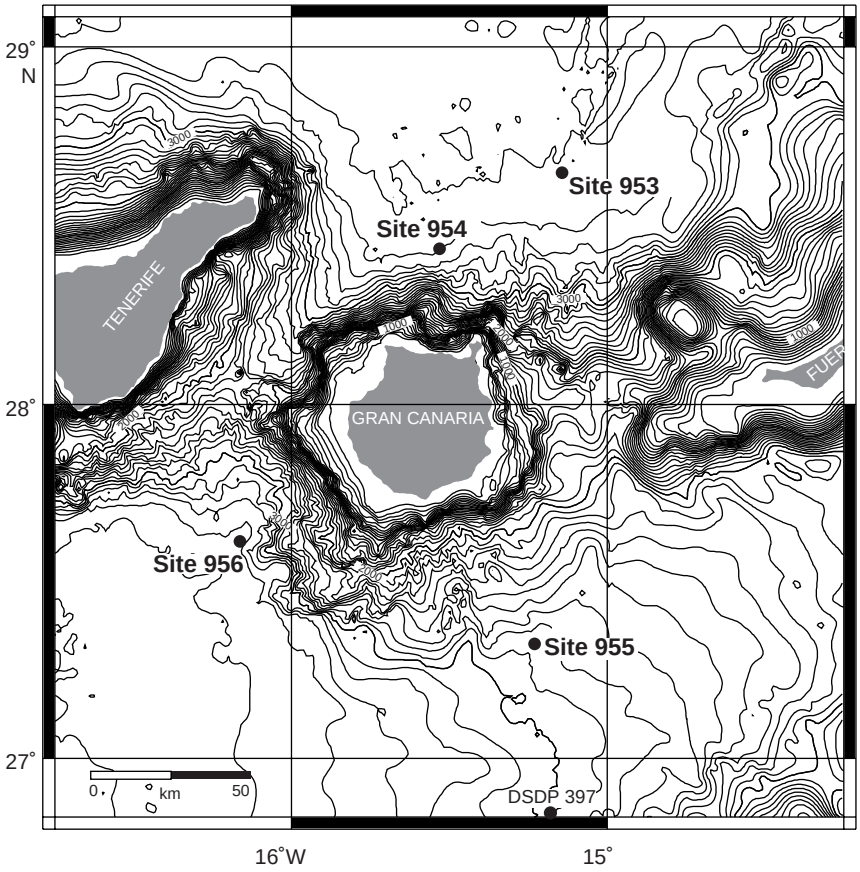

Figure 1. Locations of the drill sites located at the central Canary Islands (Schmincke, Weaver, Firth, et al., 1995).

the bottom of the lowermost debrite was not recovered (Schmincke, Weaver, Firth, et al., 1995; Schmincke and Segschneider, Chap. 12, this volume). The boundaries of these three debrites can be clearly seen in the wireline logs (Fig. 3). The debrites show graded bedding and the grain size decreases upward. The lower part of the debrite is characterized by large basaltic clasts visible in the FMS images (Fig. 5). The section below 648.4 mbsf contains a number of clasts and is characterized by specific ranges of log properties: low neutron porosity (NPHI) <46%, high density (RHOB) >2.3 g/cm^3, and high electrical resistivity in the spherically focused resistivity measurement (SFLU) of 4–9 Ωm. Between 648.4 and 620.5 mbsf, the log responses change markedly: the neutron porosity increases to values >47%, the density decreases to values <2.1 g/cm^3, and the resistivity decreases to values <2.5 Ωm. The FMS images confirm this lithologic change in the debrite, displaying a more fine-grained and homogeneous character at the top of the debrite (Fig. 6). Trends in the logs are similar in the upper debrite (615–584 mbsf).

The total magnetic field log, measured with a three-axis, flux-gate magnetometer within the General Purpose Inclinometry Cartridge (GPIT) sonde, included in the FMS tool string, provides additional information for log interpretation, although it is not calibrated absolutely. In Hole 956B, anomalies in the measurements of the magnetic field correlate with the different clast sizes in the basaltic debrites (Fig. 7). The bases of the two lowermost identified debrites consist of massive basaltic breccias and lapillistone, whereas the upper part mainly consists of basaltic hyaloclastite tuff and lapillistone. In the magnetic measurements, high frequency variations of relatively high amplitude can be seen at the base of the debrites, from 598 to 616.5 mbsf and 658 to 690 mbsf. Toward the top of each debrite, the log values become nearly constant. The topmost debrite does not contain basaltic breccia, and this may be the reason why the debrite does not produce any anomaly in the magnetic measurements.

COMPARISON OF FELSIC VOLCANICLASTIC DEPOSITS

The potassium log can be used for the identification of felsic volcaniclastic sediments for Holes 953C, 955A, and 956B (Fig. 8). Therefore, the logs are shaded for K_2O concentrations >2.1 wt%. In general, the log-derived identification of volcanic material is similar to that found in cores. The transition from the Gran Canaria basaltic shield deposits to the evolved tephra layers of the Mogán phase is best seen in Hole 956B and is clearly marked by a sharp boundary in the K_2O log. The basaltic detritus shows a low potassium content, whereas the overlying felsic volcaniclastics have a higher potassium content. However, high K_2O contents in the logs cannot always be related directly to single tephra layers; this is especially the case in Hole 953C. Between 400 and 500 mbsf, high K_2O contents are visible in the logs, whereas the core description provides only little evidence for high quantities of tephra layers. In this depth interval, the cores mainly consist of reworked pelagic sediment with high amounts of dispersed ashes (Schmincke, Weaver, Firth, et al., 1995). Thus, the abundances of volcaniclastic material are reflected in the relatively extensive depth intervals of the increased potassium contents of the logs. In contrast, the depth interval from 500 to 720 mbsf shows many thin but distinct peaks in the K_2O log. Detailed investigations of the core descriptions can link these peaks to very thin but single tephra layers that do not exceed thicknesses of 2–3 cm. The tephra layers very frequently occur in short distances, and their summation produces a distinct peak in the K_2O log. In Hole 955A, the K_2O log does not exceed 2.1 wt%. Generally, at Site 955, the ashes are highly intermixed with the pelagic sediments in beds not exceeding a few centimeters in thickness (Schmincke, Weaver, Firth, et al., 1995), therefore they do not greatly affect the potassium log.

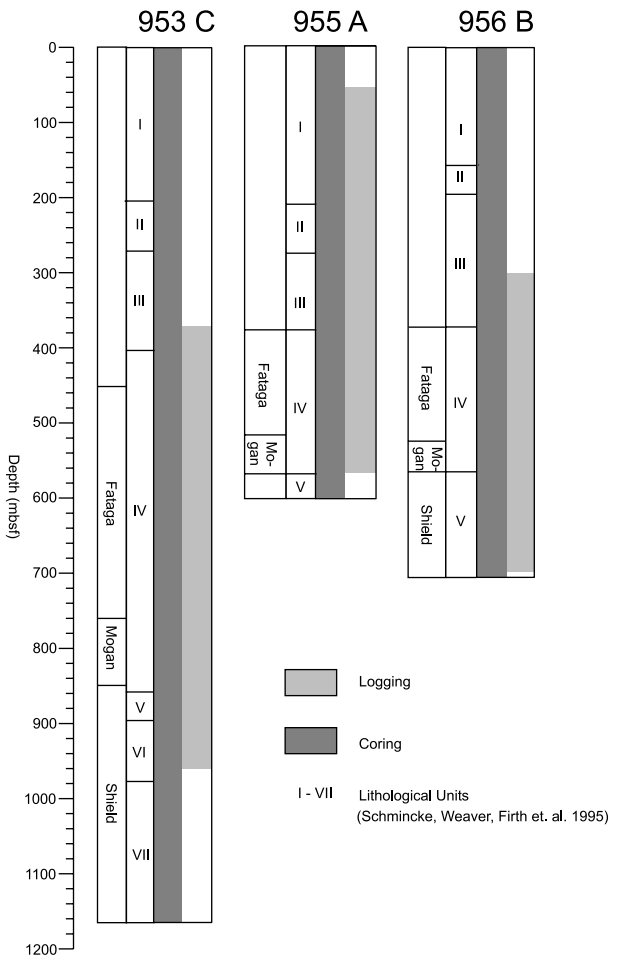

Logging Program

	NGT	DIT	SDT	HLDT	CNT-G	GLT	FMS
953C	X	X	X	X	X		
955A	X	X	X	X	X	X	X
956B	X	X	X	X	X	X	X

Figure 2. Summary of logging completed at three sites during Leg 157. NGT = natural-gamma spectrometry logging tool, DIT = dual induction tool, SDT = sonic digital logging tool, HLDT = high-temperature lithodensity tool, CNT-G = dual porosity compensated neutron tool, GLT = geochemical logging tool, and FMS = Formation MicroScanner.

RESULTS AND DISCUSSION

Volcanic deposits drilled during Leg 157 can be divided into mafic and felsic deposits. Although the shield stage is represented almost completely by basaltic material, the overlying Mogán and Fataga phases are characterized by sequences of pelagic sediments alternating with felsic and minor basaltic volcaniclastics.

The volcaniclastic deposits are identifiable by the geochemical logging data. The highly differentiated tephra layers are characterized by the highest K_2O content, whereas the basaltic volcaniclastics show the highest FeO values. The admixture of biogenic carbonate and siliciclastic sediment modify the bulk composition. The comparison of the K_2O log at all three drill sites (Fig. 8) shows that the potassium log in Holes 953C and 956B indicates more abundant tephra layers and a higher total amount of felsic volcanic material than derived from the core analysis, as reflected in the low core recovery in these two holes in depth intervals where high K_2O values are seen in the logs. Thus, the logging data suggest that the tephra layers may have been undersampled because of difficulty in recovering these generally coarser grained layers. This is confirmed by the FMS images and the core description (Schmincke, Weaver, Firth, et al., 1995). The most prominent and thickest tephra layers occur in Hole 956B. The tephra layers are clearly evident in the cores, as well as in the logging data. Sumita and Schmincke (Chap. 15, this volume) found sideromelane and hyaloclastites within the felsic ash layers that correspond to the Mogán stage volcanism. However, these basaltic fragments do not seem to appear in high amounts, because the logs show that deposition of basaltic-rich volcaniclastics starts during Fataga stage volcanism (Fig. 3). The low K_2O log values in Hole 955 are consistent with the almost complete lack of thick prominent tephra layers. The tuffitic material seems to be more dispersed in this hole, with only a few distinct tephra layers identified in the cores.

The characteristic features of the sites are related to their particular location and deposition history. In Hole 955A, the influence and input of the upwelling sediments is highest (Schmincke, Weaver, Firth, et al., 1995; Littke et al., Chap. 21, this volume). At Site 953, the farthest from Gran Canaria, ~400 m of felsic volcaniclastic sediments was deposited, whereas the occurrence of volcaniclastic sediments at Site 956 is limited to 180 m. The difference between Sites 953 and 956 is that Site 953 is situated on a flat area where the turbidity currents lost their energy and deposited the material in the suspension, whereas Site 956 is situated at the slope of the volcano (Schmincke and Sumita, Chap. 16, this volume).

Deposits of basaltic debris flows in Hole 956 can be characterized by the logging data. The base of a debrite, revealing large single clasts, is represented by low porosities, high densities, and high variations in the magnetic field. Compared to the base, the upper part of the flow is more fine grained, and the logs show higher porosities, lower densities, and an almost constant value for the magnetic field. Here, titanomagnetite is the magnetic mineral that is mainly responsible for the magnetization of the rocks (B. Herr, pers. comm., 1996). One possible reason for the variation in the magnetic log is that the remanent magnetization of large single clasts can be detected, whereas the direction of the remanent magnetization of the fine-grained components is, on average, statistically zero. Although the GPIT is designed to define the orientation of the tool, the measurements of the total magnetic field at Site 956 provided by this tool can be used for log interpretation. The resulting magnetic log is well suited to distinguish between fine- and coarse-grained basaltic fragments. In further drill holes, the general utilization of this log for lithologic interpretations should be checked.

ACKNOWLEDGMENTS

The authors are grateful to Atlas Wireline Services, Western Atlas International, Inc., for supporting us with log interpretation software. For critical review that substantially improved this paper we thank Peter Harvey and Carlos Pirmez. We also thank Hans-Ulrich Schmincke and Mari Sumita for helpful suggestions and core data. Anne Bartetzko, Renate Pechnig, and Malte Ibs-von Seht are acknowledged for several discussions and constructive comments. We are grateful to the Deutsche Forschungsgemeinschaft for financial support (grant: Wo 159/10) and ODP for providing the logging data.

REFERENCES

McDougall, I., and Schmincke, H.-U., 1977. Geochronology of Gran Canaria, Canary Islands: age of shield-building volcanism and other magmatic phases. *Bull. Volcanol.*, 40:1–21.

Schmincke, H.-U., 1976. The geology of the Canary Islands. *In* Kunkel, G. (Ed.), *Biogeography and Ecology in the Canary Islands:* The Hague (W. Junk), 67–184.

Schmincke, H.-U., 1982. Volcanic and chemical evolution of the Canary Islands. *In* von Rad, U., Hinz, K., Sarnthein, M., and Seibold, E. (Eds.), *Geology of the Northwest African Continental Margin:* Berlin (Springer), 273–306.

Schmincke, H.-U., Weaver, P.P.E., Firth, J.V., et al., 1995. *Proc. ODP, Init. Repts.*, 157: College Station, TX (Ocean Drilling Program).

Date of initial receipt: 1 July 1996
Date of acceptance: 28 August 1997
Ms 157SR-137

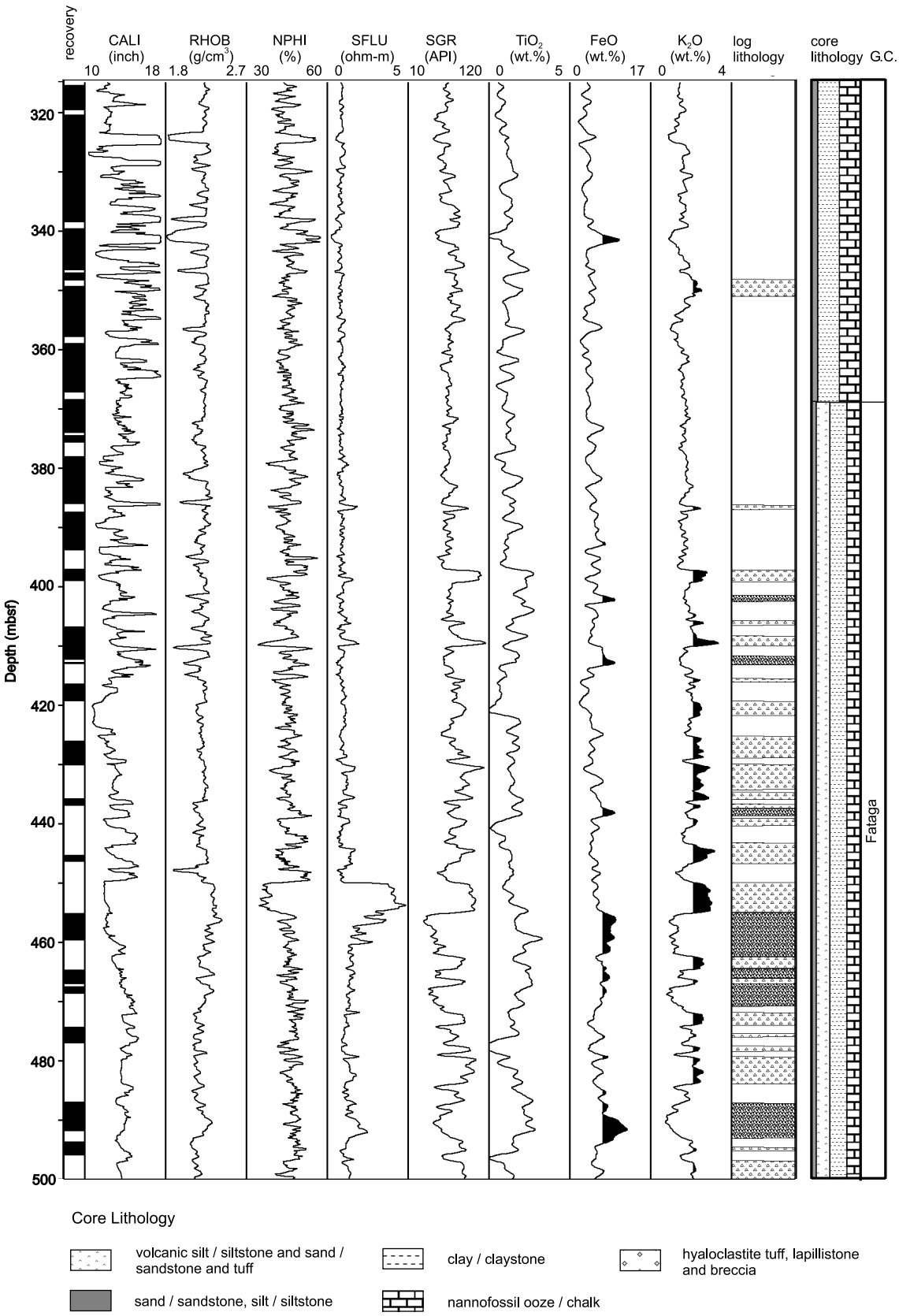

Figure 3. Discriminant logs for volcaniclastic layers in Hole 956B. The basaltic and felsic volcaniclastic sediment layers are indicated. The generalized graphic core description and phases of volcanic activity on Gran Canaria (GC) are after Schmincke, Weaver, Firth, et al. (1995).

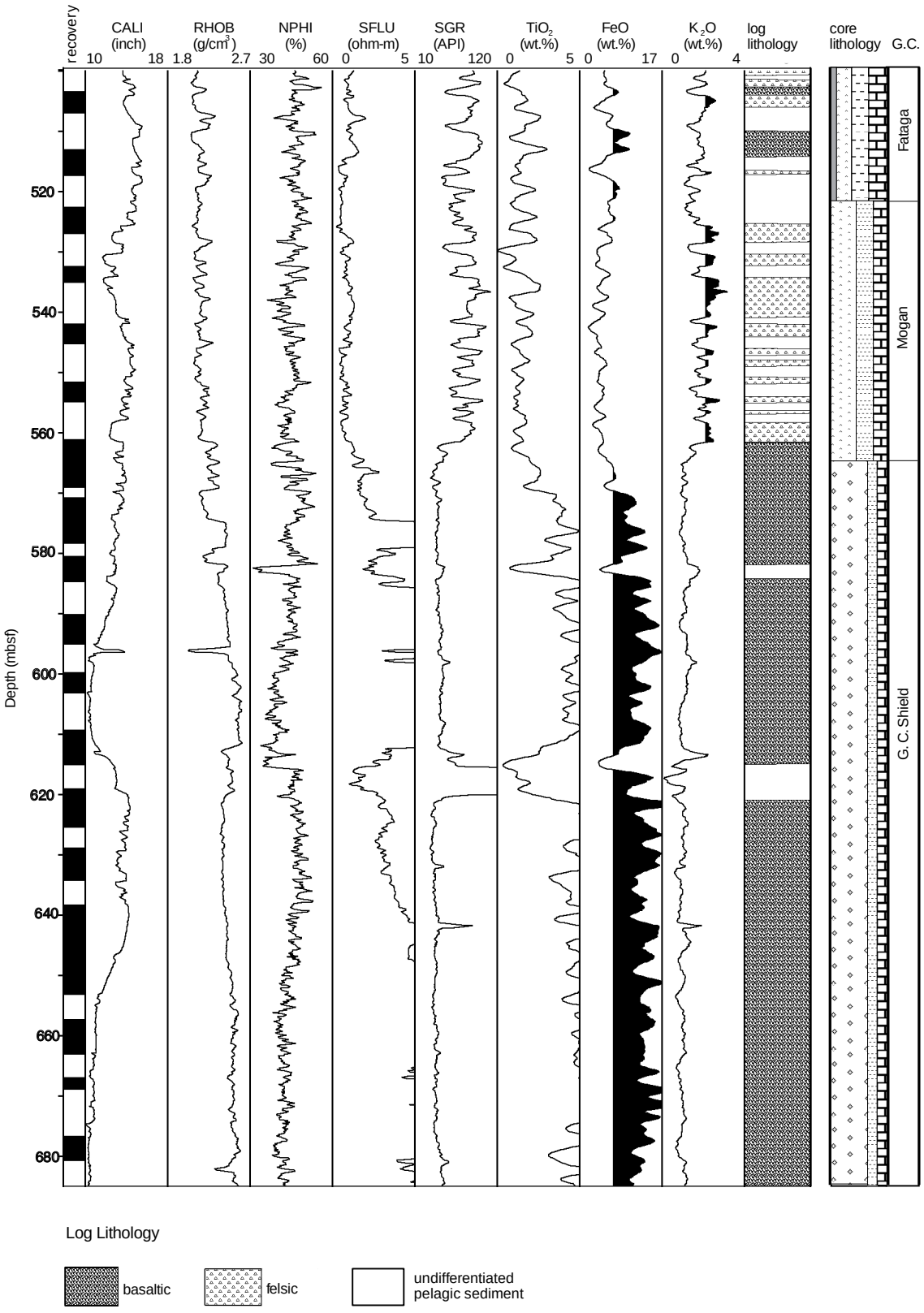

Figure 3 (continued).

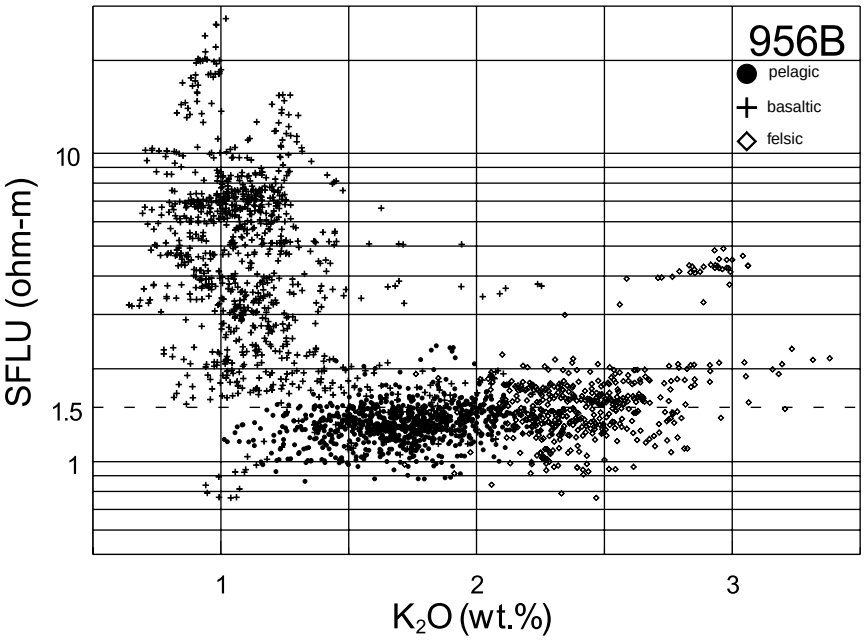

Figure 4. Crossplot of K_2O vs. the electrical resistivity SFLU differentiating pelagic, felsic, and basaltic components.

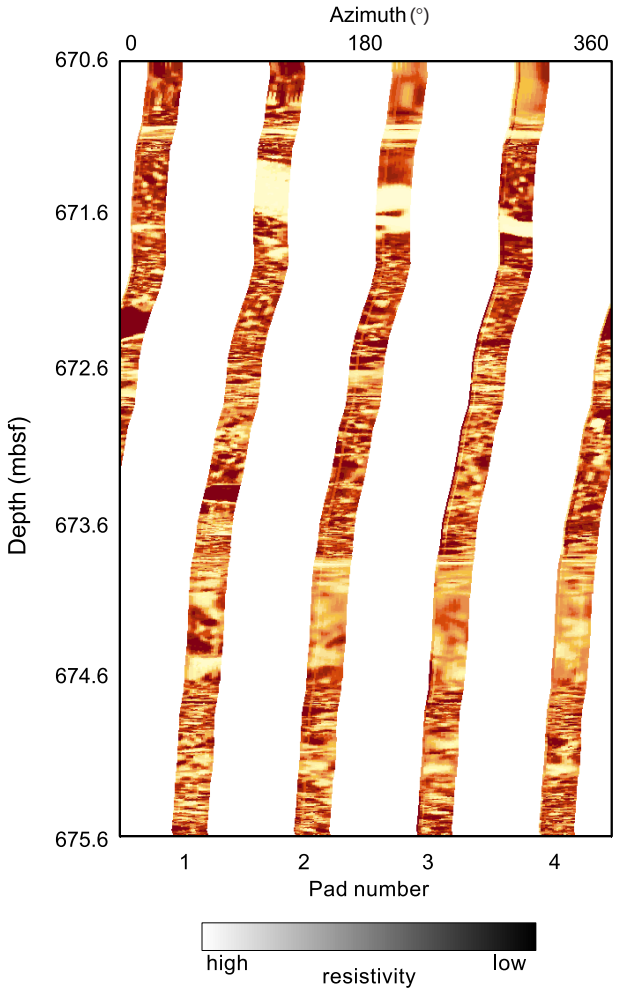

Figure 5. FMS image (670.6–675.6 mbsf) of the clast-rich base of the lowermost debrite in Hole 956B.

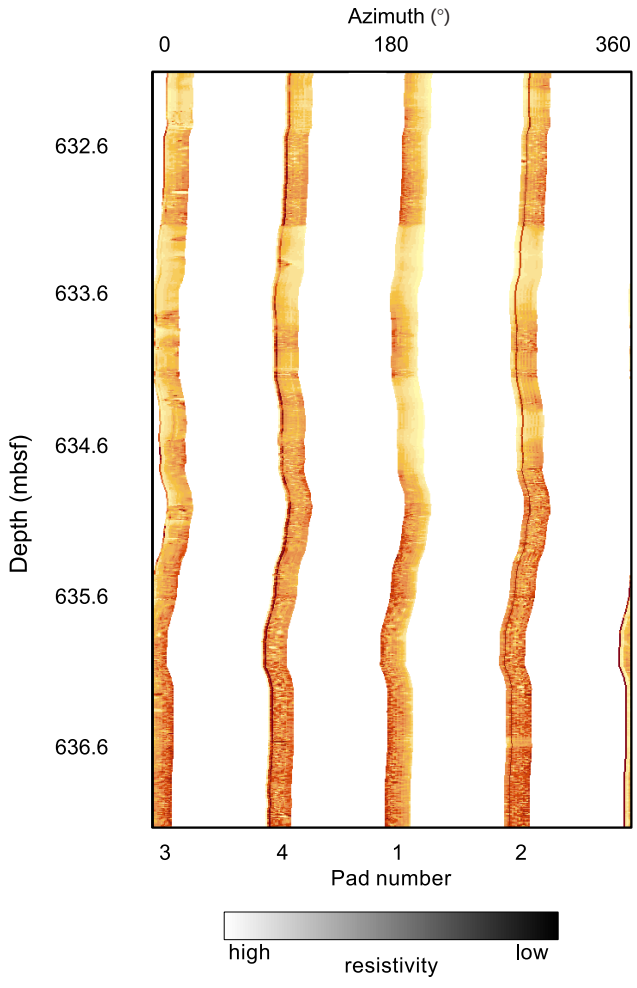

Figure 6. FMS image (631.6–641.6 mbsf) of the more homogeneous upper part of the lowermost debrite in Hole 956B.

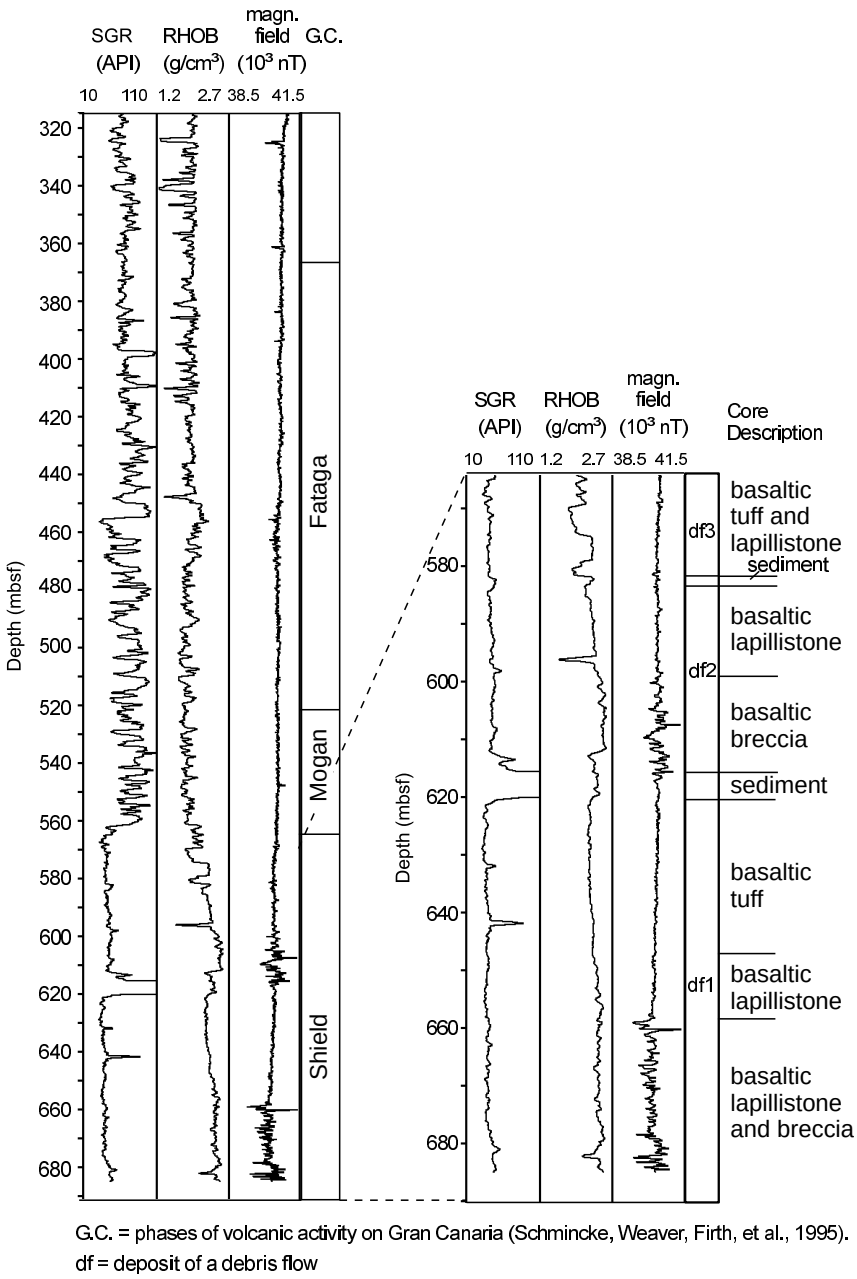

G.C. = phases of volcanic activity on Gran Canaria (Schmincke, Weaver, Firth, et al., 1995).
df = deposit of a debris flow

Figure 7. Composite log, including the total gamma ray (SGR), density (RHOB), and intensity of the magnetic field in Hole 956B. The boundaries of the debris flows are derived from the logs. The designation of the lithologies results from the core descriptions (Schmincke, Weaver, Firth, et al., 1995).

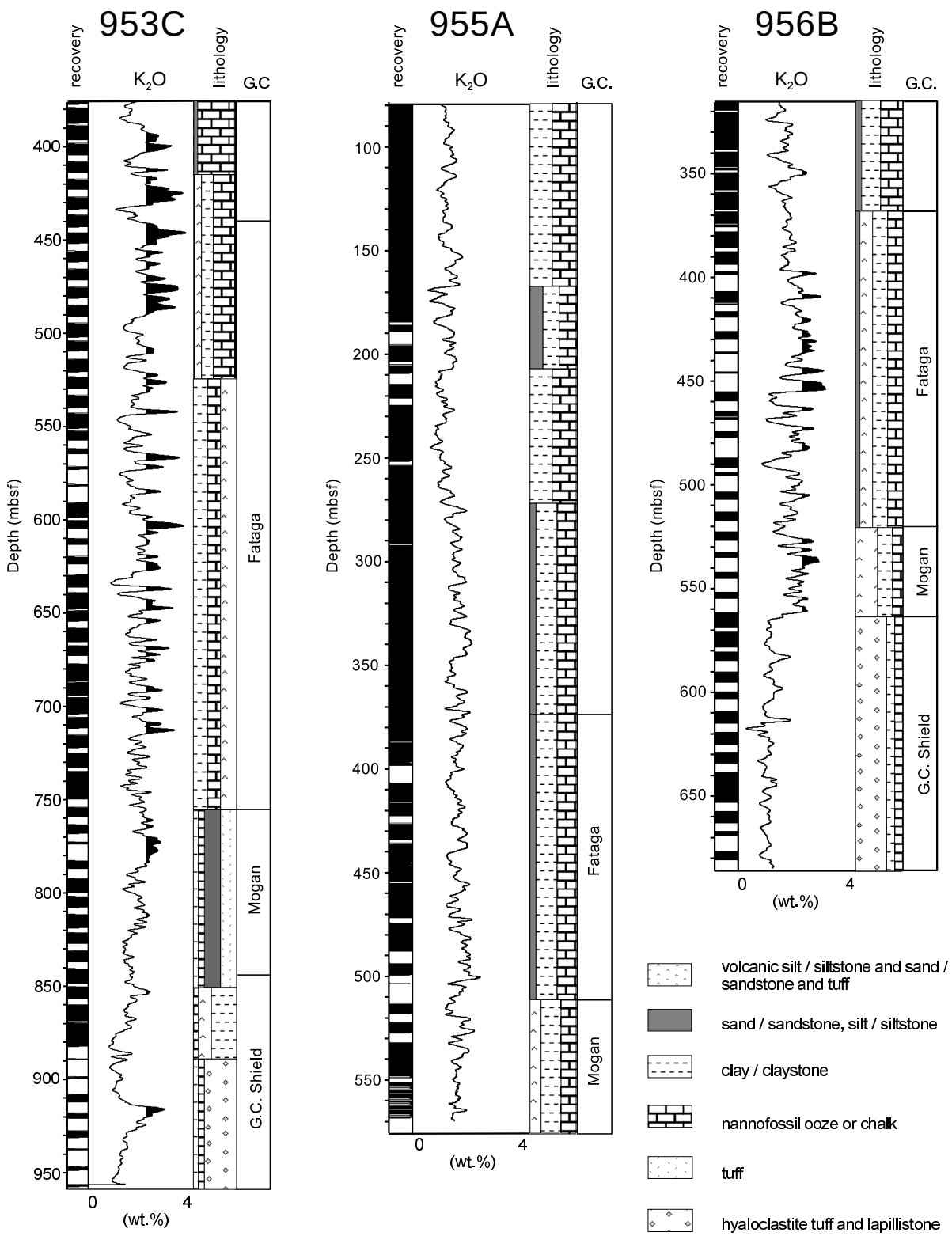

G.C. = phases of volcanic activity on Gran Canaria (Schmincke, Weaver, Firth et al., 1995).

Figure 8. Logs of the K_2O content in Holes 953, 955A, and 956B. The volcaniclastic layers with K_2O values >2.1 wt% are shaded. On the left, the core recovery is displayed, and on the right of the logs, the lithologic summary shows a generalized graphic core lithology (Schmincke, Weaver, Firth, et al., 1995).